The Combination of Finite-Length Geometric Equalization and Bandwidth Optimization for Multicarrier Transceivers

Naofal Al-Dhahir*and John Cioffi
Information Systems Laboratory
Stanford University, Stanford CA 94305

Abstract

A bandwidth–optimized and equalized multicarrier transceiver that achieves near–optimum performance at a practical complexity level is described. The equalizer used is a relatively short FIR filter whose taps and delay are set to optimize the performance of the multicarrier transceiver.

Simulation results on a set of carrier–serving–area subscriber loops are also presented to demonstrate the separate and joint effects of bandwidth optimization and equalization on performance.

Finally, the intriguing idea of using a pole–zero equalizer to achieve the high performance of infinite–complexity FIR equalizers at a much lower implementation cost is investigated.

1. Introduction

The Discrete Multitone (DMT) transceiver has attracted considerable attention recently as a viable technology for high–speed transmission on spectrally–shaped channels. Briefly, a DMT modem uses an N–point Fast Fourier Transform (FFT) to partition the channel spectrum into $\bar{N}$ ($\leq \frac{N}{2}$) parallel, independent, and memoryless subchannels. To ensure the optimality of the IFFT/FFT basis vectors as modulating/demodulating vectors (at least for the case of white noise), each input block of size N is cyclically–extended so that the input sequence looks periodic to the channel. The length of this cyclic prefix is equal to the channel memory, hence its associated bit rate loss becomes more significant for highly–dispersive channels and moderate input blocklengths.

Two of the most crucial elements in a successful design of a DMT modem are bandwidth optimization algorithms and the time–domain equalizer (TEQ).

Bandwidth optimization algorithms [1] use the signal–to–noise ratio (SNR) profile across the entire Nyquist bandwidth to determine the optimum number of subchannels that should be used out of the $\frac{N}{2}$ available ones, and the number of input bits allocated to each usable subchannel. The variability of the bit allocation profile across the subchannels coupled with the computational efficiency and accuracy by which the optimal transmission bandwidth can be determined are distinctive features of multitone modulation.

The TEQ is an FIR linear equalizer that reduces the DMT's cyclic prefix overhead by optimally shortening channel memory. The main advantage of the TEQ is that by reducing the cyclic prefix size, we can use a smaller size FFT to perform the modulation and demodulation functions, thus reducing the complexity and latency of the DMT transceiver significantly.

We showed in [2] that setting the TEQ taps to maximize the geometric SNR (denoted by SNR_{geom}) of the resulting target impulse response (TIR) results in a better DMT performance than that achieved with the TEQ of [3] that minimizes the mean square error between the equalized channel impulse response (CIR) and the TIR. However, in [2], we did not optimize the transmission bandwidth of the DMT.

Our objective in this paper is to investigate the combination of bandwidth optimization algorithms with the geometric TEQ for DMT transceivers. Our main motivation is to ascertain the feasibility of approaching the theoretical performance limits set by an infinite–blocklength DMT using a *fully–optimized* finite–complexity DMT.

2. Equalized Multicarrier Transceivers

2.1 Overview of Equalized DMT

We shall start by summarizing the main results of [2] related to the computation of the geometric TEQ.

Denote the length–N_f geometric TEQ and the length–(N_b+1) TIR by the column vectors $\mathbf{w}$ and $\mathbf{b}$, respectively. Then, we showed in [2] that their optimum tap settings are determined by solving the constrained non–linear optimization problem

$$\mathbf{b}_{opt.} = argmax\{\sum_{i=1}^{\bar{N}} \ln(\mathbf{b}^* \mathbf{G}_i^{(N_b+1)} \mathbf{b})\}\,, \qquad (1)$$

*N. Al-Dhahir is now with GE R & D Center, Schenectady, NY 12309.

0-7803-2431-5/95 $4.00

$$\text{subject to,} \quad \mathbf{b}_{opt.}^{*}\mathbf{b}_{opt.} = 1 \qquad (2)$$

$$\mathbf{b}_{opt.}^{*}\mathbf{R}_{\Delta}\mathbf{b}_{opt.} \leq MSE_{max}\,, \qquad (3)$$

where $(.)^*$ denotes the complex conjugate transpose and MSE_{max} is the maximum acceptable equalization mean square error. The number of usable subchannels, $\bar{N}$, is determined using bandwidth optimization algorithms (see Section 2.2).

The matrices $\mathbf{G}_i^{(N_b+1)}$ and $\mathbf{R}_{\Delta}$ in (1) and (3) are defined by

$$\mathbf{G}_i^{(N_b+1)} \stackrel{def}{=} \begin{bmatrix} 1 & e^{j\frac{2\pi}{N}i} & \cdots & e^{j\frac{2\pi}{N}iN_b} \\ e^{-j\frac{2\pi}{N}i} & 1 & e^{j\frac{2\pi}{N}i} & \vdots \\ \vdots & \ddots & \ddots & \ddots \\ e^{-j\frac{2\pi}{N}iN_b} & \cdots & e^{-j\frac{2\pi}{N}i} & 1 \end{bmatrix}$$

$$\mathbf{R}_{\Delta} \stackrel{def}{=} \begin{bmatrix} \mathbf{0}_{(N_b+1)\times\Delta} & \mathbf{I}_{N_b+1} & \mathbf{0}_{(N_b+1)\times s} \end{bmatrix} \mathbf{R}_{x/y}^{\perp} \begin{bmatrix} \mathbf{0}_{\Delta\times(N_b+1)} \\ \mathbf{I}_{N_b+1} \\ \mathbf{0}_{s\times(N_b+1)} \end{bmatrix},$$

where $\mathbf{I}_{N_b+1}$ is the identity matrix of size (N_b+1), $\mathbf{R}_{x/y}^{\perp} \stackrel{def}{=} (\frac{1}{S_x}\mathbf{I}_{N_f+\nu} + \mathbf{H}^*\mathbf{R}_{nn}^{-1}\mathbf{H})^{-1}$, Δ is the equalizer delay ($0 \leq \Delta \leq N_f + \nu - N_b - 1$), $s \stackrel{def}{=} N_f + \nu - \Delta - N_b - 1$, S_x is the average input energy, $\mathbf{R}_{nn}$ is the N_f-dimensional noise correlation matrix, and $\mathbf{H}$ is an $N_f \times (N_f+\nu)$ Toeplitz channel matrix whose first row is $\begin{bmatrix} h_0 & h_1 & \cdots & h_\nu & 0 & \cdots & 0 \end{bmatrix}$. The geometric TEQ is subsequently computed from

$$\mathbf{w}_{opt.}^{*} = \begin{bmatrix} \mathbf{0}_{1\times\Delta} & \mathbf{b}_{opt.} & \mathbf{0}_{1\times s} \end{bmatrix} \mathbf{H}^*(\mathbf{H}\mathbf{H}^* + \frac{\mathbf{R}_{nn}}{S_x})^{-1}\,. \qquad (4)$$

2.2 Bandwidth Optimization

In [2], we did not optimize the number of usable subchannels $\bar{N}$ (or equivalently the transmission bandwidth). Rather, we assumed that the entire available (Nyquist) bandwidth is used; i.e. $\bar{N} = \frac{N}{2}$. This choice is optimum only if the sampling frequency is optimized on a per-loop basis which is clearly impractical. On the other hand, fixing the sampling frequency at some compromise value would undoubtedly result in a significant margin loss on some loops.

In practice, the sampling frequency of the DMT transceiver is chosen high enough (larger than twice the maximum anticipated transmission bandwidth of any of the loops), then bandwidth optimization algorithms are applied to optimize $\bar{N}$ on a per-loop basis. We refer the reader to [1] for more details.

Briefly, bandwidth optimization algorithms allocate bits to each subchannel according to its SNR; subchannels whose SNRs can not support a specified minimum number of bits (e.g., 2 bits for QAM) are excluded. In optimizing the bit distribution profile, several restrictions and considerations are taken into account :

- A certain performance index is optimized (such as bit rate, margin, or input power). In this paper, we fix the target bit rate and the input power level and seek to maximize the margin.
- A constant probability of error is maintained across the usable subchannels, otherwise subchannels with the worst probability of error will dominate performance.
- Because of hardware implementation considerations, the number of bits assigned to each subchannel is restricted to be an integer (or a fraction with a minimum specified granularity) that is less than a maximum allowable number of bits per subchannel (chosen to accommodate the bit precision of the digital-to-analog converter).
- A flat energy distribution is assumed over the transmission bandwidth. This assumption has been shown in [4] to be near-optimum *as long as the transmission bandwidth is optimized.*

For the equalized DMT transceiver, we need to apply the bandwidth optimization algorithms twice. The first round is needed to determine the optimum portion of the Nyquist bandwidth that should be used based on the identified channel and noise characteristics during system initialization. The geometric TEQ then equalizes this bandwidth-optimized (but still highly-dispersive) channel response into a TIR that maximizes SNR_{geom} (and is much less dispersive) over that same bandwidth. The second round of bandwidth optimization determines the number of subchannels that should be used according to the characteristics of the TIR and the new noise power spectral density (psd).[1]

3. Simulation Results

We performed extensive computer simulations to quantify the effects of bandwidth optimization on the performanace of the DMT with and without equalization. The simulation parameters are representative of the high-bit-rate digital subscriber Line (HDSL) environment. In particular, the channel impulse responses considered are those of the eight carrier-serving-area (CSA) loops depicted in Figure 1.

The noise consists of two components : an AWGN component with a two-sided psd of -113 dBm/Hz and near-end crosstalk that is modeled by the transfer characteristics $|H_{NEXT}(f)|^2 = k_{NEXT}f^{\frac{3}{2}}$ with $k_{NEXT} =$

[1] The original noise psd is filtered by the geometric TEQ.

10^{-13}. The sampling frequency, target bit rate, and the input power level are fixed at 640 kHz, 800 kbps, and 14 dBm, respectively. The probability of symbol error is assumed equal to 10^{-7} and a coding gain of 4.2 dB is included. The DMT blocklength is 128, the length of the geometric TEQ is $N_f = 16$, and the length of the TIR, $(N_b + 1)$, is fixed at 5 samples. In arriving at the optimum TIR settings, we always started with the initial condition of the unit–norm all–ones vector.

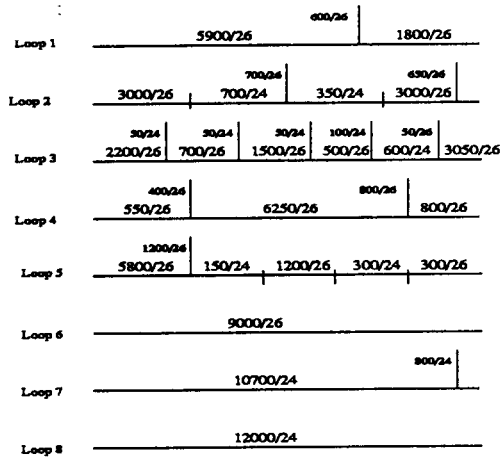

Figure 1: Configuration of the 8 CSA HDSL loops under study (length (in ft.)/gauge)

In [2], we fixed MSE_{max} at -17 dB and further assumed that the delay of the geometric TEQ is equal to to the optimum delay of the MMSE–TEQ. Here, we allow a slight variation in MSE_{max}. according to the loop characteristics with the objective of optimizing performance.

In Figure 2, we have plotted the achievable DMT margin with and without bandwidth optimization and with and without the geometric TEQ. For the sake of comparison, we have also calculated the DMT margin under the assumptions of infinite blocklength and optimized bandwidth; this case constitutes a performance upperbound.

Comments :

- It is clear from Figure 2 that bandwidth optimization offers an appreciable improvement in margin, the amount of which varies from loop to loop.
- The combination of the geometric TEQ and bandwidth optimization brings the margin very close (within 2-3 dB on most loops) to theoretical performance limits.
- The remaining margin gap with respect to the infinite blocklength case is mainly due to the finite–length constraint imposed on the TEQ and the

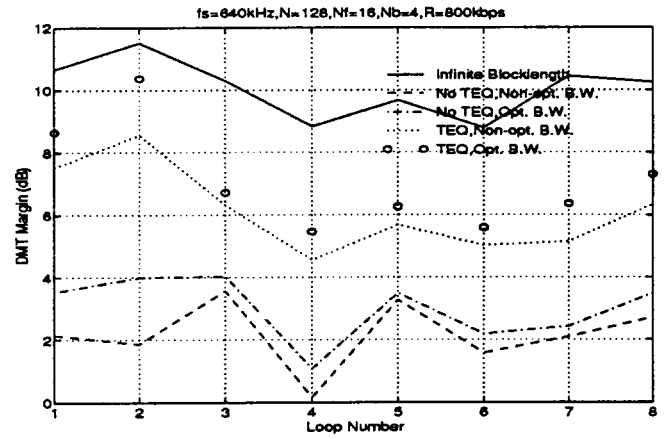

Figure 2: DMT margin for the 8 CSA loops w/ and w/o equalization and w/ and w/o bandwidth optimization

DMT blocklength. Next, we shall illustrate the additional margin improvement that can be gained by increasing the TEQ length.

4. A Pole-Zero Geometric TEQ

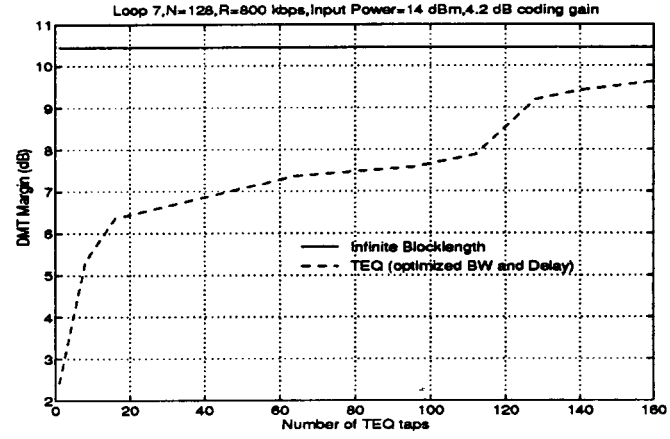

Figure 3: Variation of the DMT margin with the TEQ length for Loop 7

To demonstrate the performance improvement that can be achieved by increasing the length of the geometric TEQ, we have plotted in Figure 3 the variation of DMT margin with N_f for Loop 7.

However, a real–time implementation of this 128–tap TEQ is very costly because of the high processing power and large memory needed, especially as the sampling frequency is further increased to accommodate higher target bit rates.

To reduce implementation cost, we propose to use the algorithm that we derived in [5] to model the long

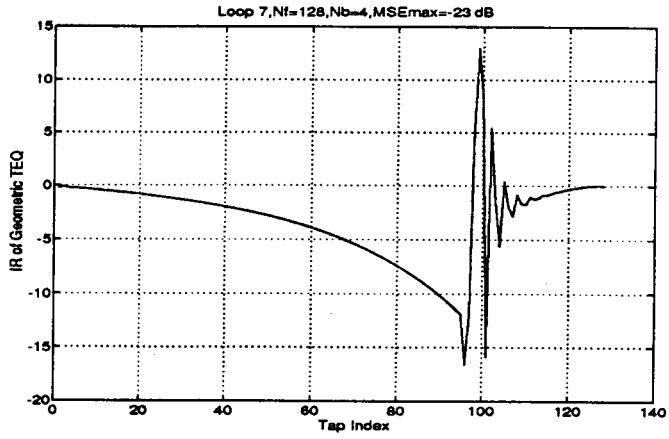

Figure 4: IR of the optimum geometric TEQ of length 128 for Loop 7

FIR TEQ by a stable pole–zero TEQ with much fewer taps. We conclude this section by an example that illustrates the performance of this algorithm.

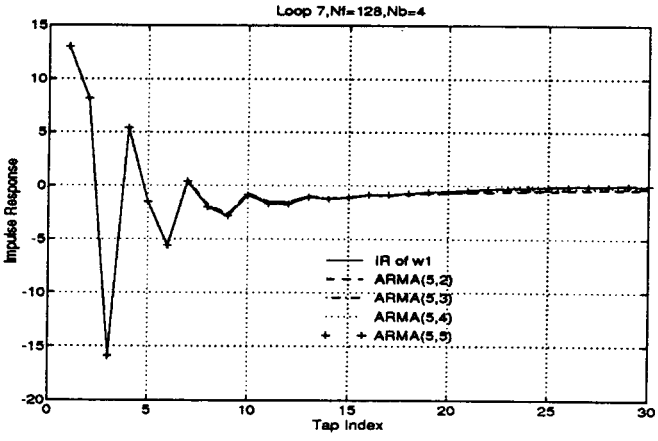

Figure 5: IR of $w_1(D)$ together with its pole–zero approximations

Example 1 *Using the same simulation parameters of Section 3 and setting $N_f = 128$ and $MSE_{max} = -23$ dB, the impulse response (IR) of the optimum geometric TEQ for Loop 7 is shown in Figure 4.*

To facilitate the pole–zero modeling task of this IR, we shall use the "splitting" technique described in [5]. Briefly, the IR is split at its peak sample into two IRs, then each one of them is separately approximated by a pole–zero model. The IRs of some of the best pole–zero models obtained for the post–peak, denoted by $w_1(D)$, and the pre-peak, denoted by $w_2(D)$, overlaid on the IR of the original FIR IR are plotted in Figures 5 and 6, respectively. In these figures, the notation $ARMA(p,q)$ denotes a pole–zero model with p poles and q zeros.

It is evident that the proposed algorithm generates highly–accurate pole–zero models that have much fewer taps than the original FIR filter.

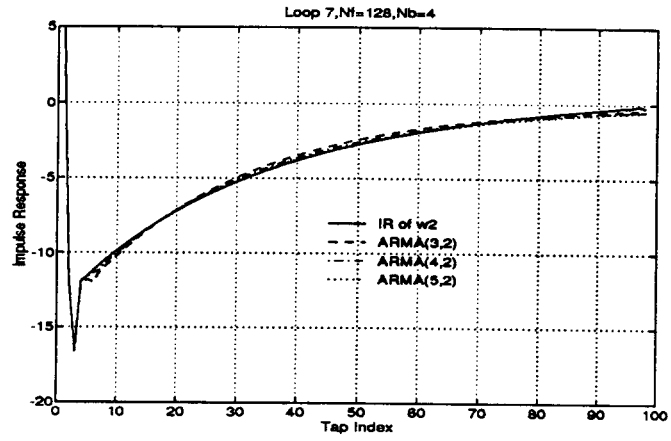

Figure 6: IR of $w_2(D)$ together with its pole–zero approximations

References

[1] P. Chow and J. Cioffi. Bandwidth Optimization for High Speed Data Transmission over Channels with Severe Intersymbol Interference. In *Global Telecommunications Conference*, pages 59–63, December 1992.

[2] N. Al-Dhahir and J. Cioffi. Optimum Finite-Length Equalization for Multicarrier Transceivers. In *Globecom Conference Proceedings, San Francisco, CA*, November 1994.

[3] J. Chow and J. Cioffi. A Cost-Effective Maximum Likelihood Receiver for Multicarrier Systems. In *International Conference on Communications, Chicago*, pages 948–952, June 1992.

[4] P. Chow. *Bandwidth Optimized Digital transmission Techniques for Spectrally Shaped Channels with Impulse Noise.* PhD thesis, Stanford University, May 1993.

[5] N. Al-Dhahir, A. Sayed, and J. Cioffi. A High-Performance Cost-Effective Pole-Zero MMSE-DFE. In *Allerton Conference on Communication, Control, and Computing*, pages 1166–1175, September 1993.